View metadata, citation and similar papers at core.ac.uk

brought to you by CORE

provided by University of Bergen

AGU PUBLICATIONS

Geophysical Research Letters

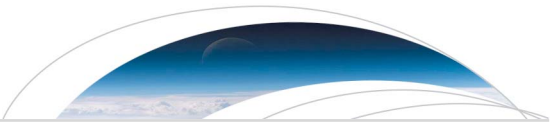

RESEARCH LETTER

10.1002/2017GL074304

Key Points:
- Record low sea ice extent in the Barents Sea in recent winters
- The current observed trend appears as an uncommon feature in observations and climate models
- Large spread in model projections of ice-free conditions due to large internal variability

Correspondence to:
I. H. Onarheim,
ingrid.onarheim@uib.no

Citation:
Onarheim, I. H., and M. Årthun (2017), Toward an ice-free Barents Sea, *Geophys. Res. Lett.*, *44*, 8387–8395, doi:10.1002/2017GL074304.

Received 1 JUN 2017
Accepted 31 JUL 2017
Accepted article online 3 AUG 2017
Published online 25 AUG 2017

©2017. The Authors.
This is an open access article under the terms of the Creative Commons Attribution-NonCommercial-NoDerivs License, which permits use and distribution in any medium, provided the original work is properly cited, the use is non-commercial and no modifications or adaptations are made.

Toward an ice-free Barents Sea

Ingrid H. Onarheim[1] and **Marius Årthun**[1]

[1]Geophysical Institute, University of Bergen and Bjerknes Centre for Climate Research, Bergen, Norway

Abstract Arctic winter sea ice loss is most pronounced in the Barents Sea. Here we combine observations since 1850 with climate model simulations to examine the recent record low winter Barents Sea ice extent. We find that the present observed winter Barents Sea ice extent has been reduced to less than one third of the pre-satellite mean and is lower than the minimum sea ice extent in all multicentury climate model control simulations assessed here. The current observed sea ice loss is furthermore unprecedented in the observational record and appears as an uncommon trend in the long control simulations. In a warming climate, projections from the large ensemble simulation with the Community Earth System Model show a winter ice-free Barents Sea for the first time within the time period 2061–2088. The large spread in projections of ice-free conditions highlights the importance of internal variability in driving recent and future sea ice loss.

1. Introduction

The loss of Arctic summer sea ice in recent decades is well documented and one of the most visible manifestations of ongoing climate change [*Serreze et al.*, 2007]. Although less dramatic and less studied, the Arctic winter sea ice cover has also displayed a steady retreat since satellite measurements of sea ice began in 1979 [*Cavalieri and Parkinson*, 2012]. These wintertime sea ice changes largely result from a retreating Barents Sea ice cover (Figure 1) [*Onarheim et al.*, 2015; *Li et al.*, 2017]. The recent decade has seen reduced sea ice growth leading to an accelerated trend toward lower Barents Sea ice extent, with the sea ice extent in 2016 and 2017 being the lowest on record (Figure 1).

The loss of sea ice in the Barents Sea can potentially affect climate and weather in lower latitudes [*Liptak and Strong*, 2014; *Sorokina et al.*, 2016], and Arctic ecosystems and fisheries [e.g., *Dalpadado et al.*, 2014]. The location of the sea ice edge in the Barents Sea also impacts shipping opportunities and offshore industry [*ACIA*, 2005]. It is therefore of great interest to understand winter sea ice variability and trends in the Barents Sea with respect to past variability and to predict the future fate of the winter sea ice cover.

The Barents Sea is a seasonally ice covered Arctic shelf sea, and a transition zone between the temperate Nordic Seas and the cold Arctic Ocean. The ocean climate in the Barents Sea is dominated by the varying influence of the Atlantic water inflow in the Norwegian Atlantic Current, a poleward extension of the Gulf Stream [e.g., *Smedsrud et al.*, 2013]. Variations in the Atlantic inflow exert a dominant influence on the variability and trend of the winter Barents Sea ice cover, by determining the amount of wintertime freezing [*Venegas and Mysak*, 2000; *Vinje*, 2001; *Årthun et al.*, 2012; *Smedsrud et al.*, 2013; *Onarheim et al.*, 2015; *Li et al.*, 2017]. Consequently, the Barents Sea ice cover displays pronounced interannual to multidecadal variability as a response to changes in the large-scale ocean circulation and associated changes in poleward ocean heat transport [*Venegas and Mysak*, 2000; *Vinje*, 2001; *Zhang*, 2015]. Low-frequency climate variability, reminiscent of the Atlantic Multidecadal Oscillation, is also evident in Barents Sea temperatures [*Skagseth et al.*, 2008; *Levitus et al.*, 2009].

The presence of substantial decadal to multidecadal sea ice variability in the Barents Sea makes it necessary to consider long time series when evaluating the uniqueness of the ongoing winter Barents Sea ice loss. Hence, in order to assess the occurrence of winter sea ice trends of varying lengths, we will combine a new observational data set covering the time period since 1850 [*Walsh et al.*, 2015, 2017] and multimodel, multicentury climate model control simulations. We also consider future trends in a warming climate, using mainly the Community Earth System Model large ensemble simulation (CESM-LE) [*Kay et al.*, 2015], to assess the possibility of ice-free

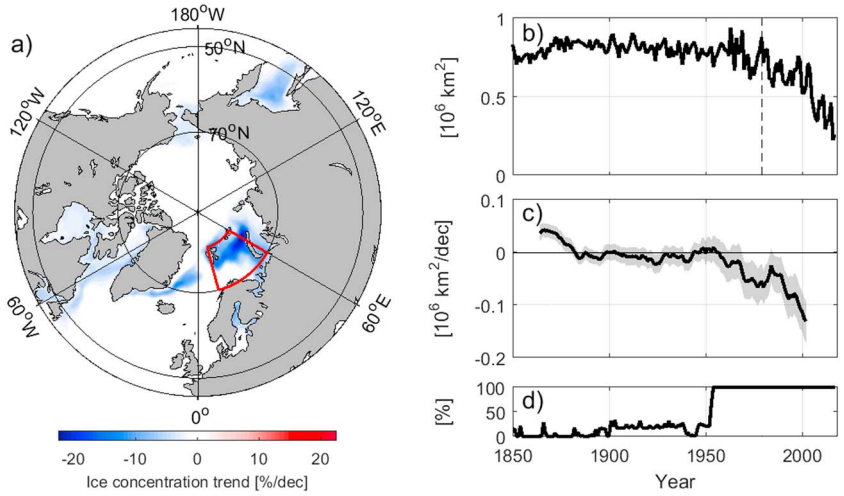

Figure 1. (a) Observed winter sea ice concentration trend, 1979–2017. The red box outlines the Barents Sea. (b) Barents Sea winter sea ice extent between 1850 and 2017. The vertical dashed line indicates the year 1979. (c) Successive 30 year trends in Barents Sea winter sea ice extent, 1850–2017. Trends are displayed at the center of each 30-year period. The gray shading indicates the 95% confidence interval. Note that the confidence interval does not take into account uncertainties with respect to data quality. d) Fraction of winter Barents Sea ice concentration data based on observations. 100% indicates that no data is based on analogs or interpolation by *Walsh et al.* [2015].

conditions in the Barents Sea in winter toward the end of the century. This study thus provides the first detailed assessment of past, present, and future trends in observed and modeled Barents Sea winter sea ice extent.

2. Data and Methods

To assess and quantify Barents Sea ice variability and trends, we use a new data set of observed sea ice concentration spanning the time period 1850 to 2013 [*Walsh et al.*, 2015]. Sea ice concentration is satellite derived since 1979, calculated by combining concentration estimates from the Bootstrap and NASA Team algorithms [*Meier et al.*, 2013]. Prior to the satellite era, observations are compiled from, e.g., ship reports and airplane surveys [*Walsh et al.*, 2015, 2017]. To assess the most recent (2014–2017) Barents Sea ice loss, we use satellite-derived sea ice concentrations based on the NASA Team algorithm [*Cavalieri et al.*, 1996; *Maslanik and Stroeve*, 1999]. For consistency, we replace the Walsh product with the NASA Team product throughout the satellite era, 1979–2013, in the 1850 onward data set; i.e., sea ice concentrations are based on the NASA Team algorithm from 1979 to 2017. Minor differences in winter Barents Sea ice extent, 1979–2013, were found between the two sea ice products; a detrended correlation of 0.98, mean ± standard deviation of 0.64 $\pm$0.13 $\times$ 10^6 km^2 and 0.60 $\pm$ 0.14 $\times$ 10^6 km^2, and linear trends of -0.09×10^6 km^2 per decade and -0.10×10^6 km^2 per decade, for the combined (Bootstrap/NASA Team) product and the NASA Team product, respectively. The historical sea ice concentration is mid-monthly and given on a 0.25° latitude by 0.25° longitude grid, whereas the monthly satellite observations are on a 25 km by 25 km grid. The pre-satellite data clearly contain larger uncertainties with respect to trends and variability; however, this uncertainty is not quantified [*Walsh et al.*, 2017]. As a simple measure of data uncertainty, we show in Figure 1d the fraction of the winter Barents Sea ice concentration data which is based on observations, i.e., where the sea ice data is not based on analogs or interpolation by *Walsh et al.* [2015] (100% means that the sea ice concentration in each grid point is based on observations for all winter months). For a detailed description of the different data sources see *Walsh et al.* [2015]. The extended data set is nevertheless valuable for putting the recent sea ice loss into a longer historical perspective.

We consider winter (November–April; we note that results are not sensitive to the chosen definition of the winter season) sea ice extent in the area 70–81°N, 15–60°E (red box in Figure 1a), following, e.g., *Årthun et al.* [2012]. A large part of the historical observations are of the sea ice edge, making sea ice extent beneficial compared to sea ice concentration or area. Sea ice extent is calculated as the cumulative area of all grid cells where monthly mean sea ice concentration is larger than 15%. Linear trends are thereafter calculated over 10–100 year time periods, although we will mainly consider 30 year trends when discussing temporal changes in the Barents Sea ice cover [cf., *Serreze and Stroeve*, 2015].

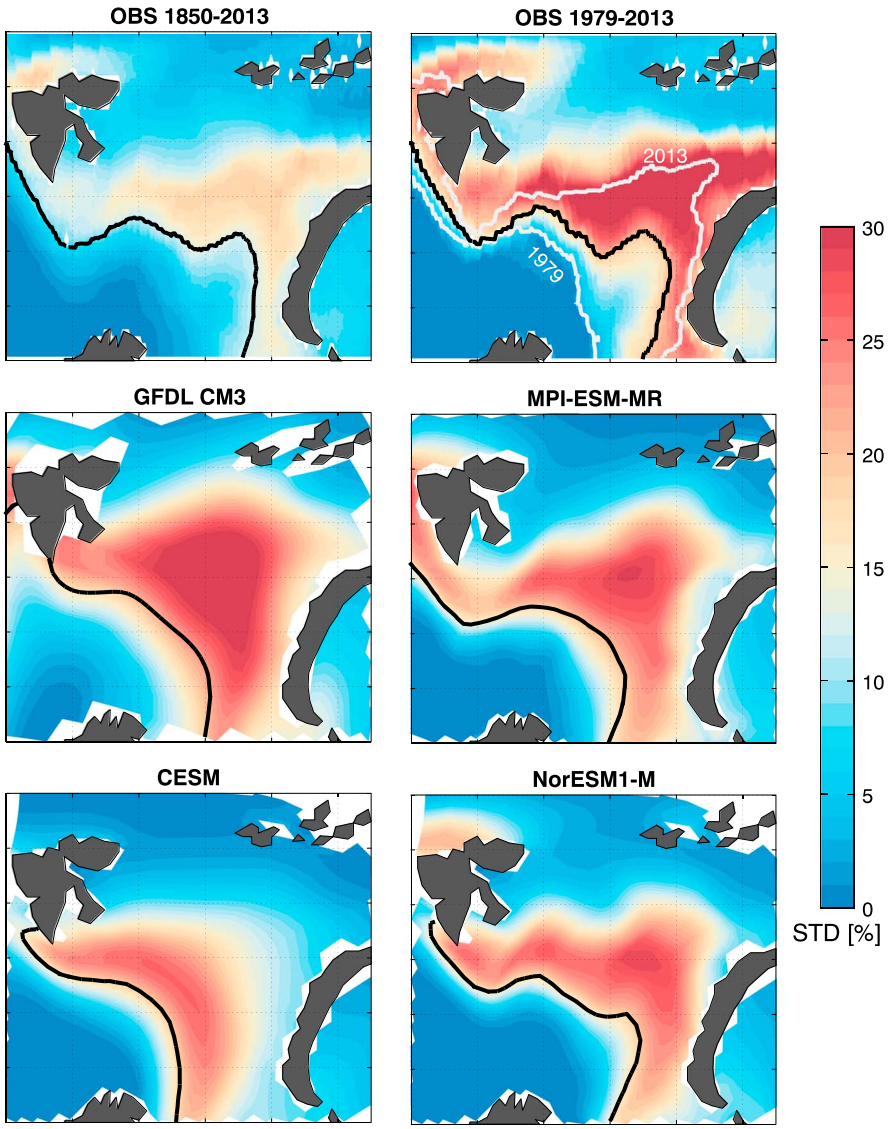

Figure 2. Standard deviation of winter sea ice concentration (colors) and mean sea ice edge (15% sea ice concentration; black contour line) in observations [*Walsh et al.*, 2015] and preindustrial climate model control simulations. Note that the data have not been detrended. The observed sea ice edge in 1979 and 2013 are also shown (white contours in the first row).

To evaluate when the Barents Sea approaches ice-free conditions, we define (nearly) ice-free conditions as 10% of the pre-satellite (1850–1978) average winter sea ice extent (0.08×10^6 km^2). This allows for a small amount of sea ice to remain during parts of the winter, although the ocean is for all practical purposes ice free.

To assess the probability of the occurrence of observed trends as a result of internal variability, we analyze preindustrial control simulations (no external forcing) from four commonly used global climate models available from the fifth phase of the Coupled Model Intercomparison Project (CMIP5) [*Taylor et al.*, 2012]; NorESM1-M [*Bentsen et al.*, 2013] (500 year simulation), GFDL CM3 [*Griffies et al.*, 2011] (500 year simulation), CESM [*Kay et al.*, 2015] (1800 year simulation), and MPI-ESM-MR [*Giorgetta et al.*, 2013] (1000 year simulation). The combination of the four control runs, 3800 years in total, is sufficient to span a broad range of internal variability [e.g., *Kay et al.*, 2011; *Li et al.*, 2017], and the full suite of CMIP5 control simulations is therefore not included here. Keeping in mind that the simulations do not include external forcing, the location of the simulated mean sea ice edge in the Barents Sea is in fairly good agreement with observations in all the models (Figure 2). Consistent with observations, the area of maximum variance in the models stretches toward the northeast along the path of the warm Atlantic water [e.g., *Årthun et al.*, 2012]. The magnitude of variability

in the models is larger than that observed if we consider the time period since 1850, while it is in better agreement with that observed during the satellite period. We note that our results are not sensitive to the differences in grid size. A detailed model evaluation is not performed here, and the reader is referred to, e.g., *Sandø et al.* [2014a] (NorESM1), *Griffies et al.* [2011] (GFDL CM3), *Jahn et al.* [2016] (CESM), and *Notz et al.* [2013] (MPI-ESM).

The same four climate models are also used to assess the future development of the Barents Sea ice cover. The simulations considered here use historical forcing for the period 1850–2005 and Representative Concentration Pathway (RCP) [*Moss et al.*, 2010] 8.5 forcing from 2006 to 2100. Instead of using a larger selection of CMIP5 models, we mainly make use of the CESM-LE, from which 40 ensemble members are available for the time period 1920 to 2100. These ensemble members all use the same Earth system model and the same external forcing but have small atmospheric initialization differences. Consequently, the CESM-LE ensemble spread is only generated by internal climate variability, unlike the CMIP5 multimodel spread that results also from different model physics. CESM-LE simulates a realistic Arctic sea ice cover and has previously been used to assess Arctic summer sea ice loss [*Swart et al.*, 2015; *Barnhart et al.*, 2016; *Jahn et al.*, 2016]. To assess scenario uncertainty, we also make use of the CESM medium ensemble (ME) [*Sanderson et al.*, 2015], which consists of 15 ensemble members forced with RCP4.5 from 2006 to 2080.

3. Observed Sea Ice Variability and Change 1850–2017

The Northern Hemisphere (NH) winter sea ice extent has linearly decreased by 1.8×10^6 km^2 since 1979, with largest trends occurring in the Barents Sea (Figure 1a). Despite the Barents Sea's relatively small area (roughly 4% of the NH's ice covered area), it contributes to 24% of the observed NH winter sea ice loss. The winter Barents Sea ice extent has decreased by 0.43×10^6 km^2 since 1979 (Figure 1b). The sea ice loss is associated with a northeastward retreating sea ice edge (Figure 2) and is particularly large in the northeastern Barents Sea (Figure 1a). As a consequence, large parts of the Barents Sea have been ice free in recent winters. The number of months with ice-free conditions has increased from less than one in the 1980s to six in 2016, and November (the first winter month) has been ice free in five of the last 8 years (not shown).

During the most recent decade the Barents Sea ice extent has been less than half of the pre-satellite (1850–1978) mean (Figure 1b). The two most recent winters have had an unprecedentedly small sea ice cover, only 28–32% of the pre-satellite mean, or 40–45% of the satellite mean. Prior to the satellite era, the Barents Sea ice cover shows large interannual variability, and less pronounced decadal to multidecadal variability. The sea ice extent increases slightly from the 1850s to the 1900s, decreases gradually to the 1950s, increases to the 1970s, and displays a rapid decline since. Consistent with *Vinje* [2001] and *Miles et al.* [2014], there is no clear signal of the 1930s early warming period. The long-term changes are reflected in successive 30 year trends (Figure 1c). The 30 year trends are generally small until the 1980s–1990s, whereas the recent trends are large and unprecedented, exceeding -0.13×10^6 km^2 per decade during the last 30 years. We note that recent 20–40 year trends are also unprecedented.

4. Sea Ice Variability and Trends in Preindustrial Control Simulations

To assess the probability of the ongoing winter Barents Sea ice loss to occur as a result of internal variability, we examine trends in preindustrial control simulations from CESM, GFDL CM3, MPI-ESM-MR, and NorESM1-M. The present observed trend is an uncommon feature in these models (Figure 3). The probability of a simulated 30 year trend to be larger than or equal to the most recent observed 30 year trend is less than 0.1% in MPI-ESM-MR, NorESM1-M, and CESM, and slightly higher (2%) in GFDL CM3 (Figure 3). We note that trends are not scaled by the mean sea ice extent in the individual models, but that the results are consistent if we consider a percentage trend. The observed sea ice extent in recent years is also an uncommon feature in the control simulations; the observed sea ice extent in 2016 and 2017 is outside the range of variability in all the preindustrial control simulations considered here (horizontal dashed lines in Figure 4a).

In three out of the four models, the simulated 30 year trends are generally less than half of the current observed trend. The GFDL CM3 simulation has larger trends than the other models and has 30 year trends larger than that observed ten times during the 500 year model run. Hence, according to these models, the chance of the recent observed trend to occur is small in a simulated preindustrial climate. In contrast, the observed decadal trends are less rare in the model simulations, e.g., the probability of a simulated 10 year trend to be larger than or equal to the current observed 10 year trend is 6–25% in all models (not shown). Figure 3 furthermore

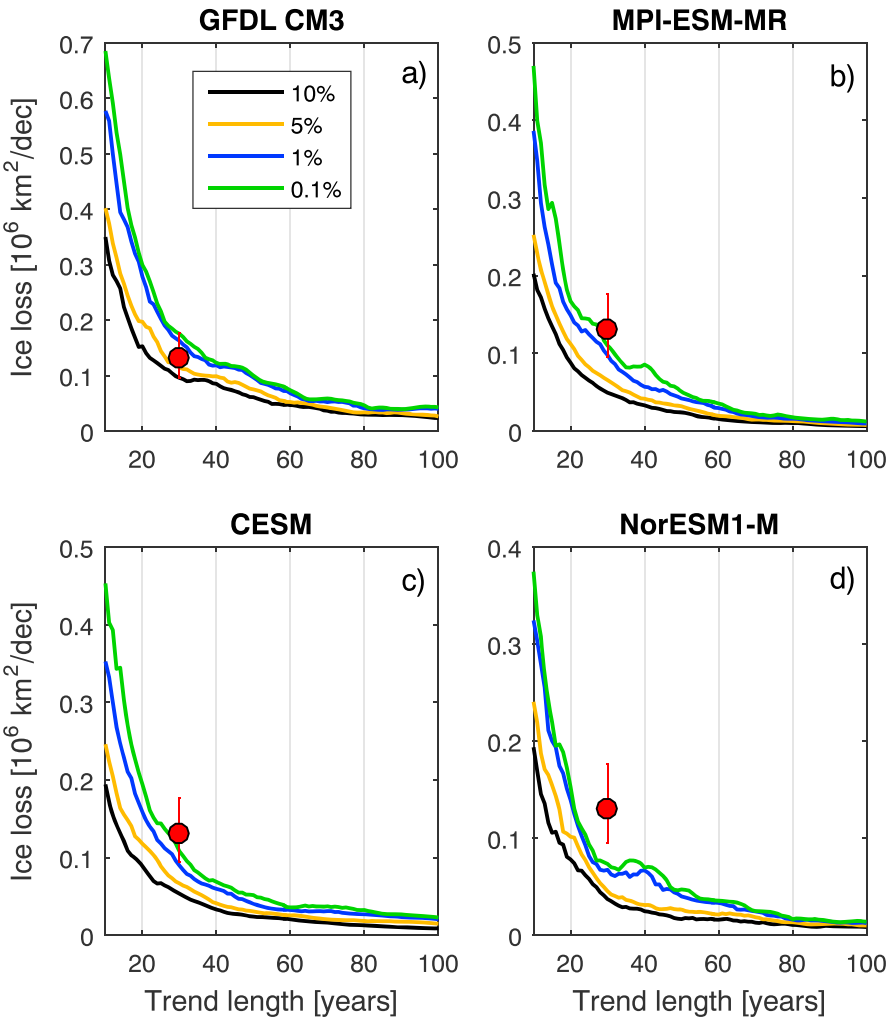

Figure 3. The probability (%) of a winter Barents Sea ice extent trend with a specified length (10–100 years) and magnitude to occur in preindustrial control simulations by (a) GFDL CM3, (b) MPI-ESM-MR, (c) CESM (c), and (d) NorESM1-M. Red dots indicate the most recent observed 30 year trend, and corresponding bars show the 95% confidence intervals. Note the different scales on the *y*-axes.

illustrates that the probability for large trends to occur increases for decreasing time intervals over which the trend is calculated, i.e., the largest trends occur for the shortest time intervals.

5. Future Barents Sea Ice Cover

The rapidly shrinking winter Barents Sea ice cover may portend that the Barents Sea is going toward ice-free conditions year round. As a simple estimate of when ice-free winter conditions may occur, we calculate linear and quadratic trends over the most recent 30 year period (1988–2017; both being good fits for the recent observed sea ice evolution) and then extrapolate the trends into the future. This method suggests ice-free conditions in 2023 and 2036 for quadratic and linear trends, respectively. We note that these statistical projections are highly uncertain as they are only based on extrapolating the observed trend and assume that the current sea ice extent trend prevails [e.g., *Meier et al.*, 2007].

To further investigate the future fate of the Barents Sea ice cover in the presence of climate change, we mainly employ the CESM-LE simulation, and also future climate change simulations (single realizations) from GFDL CM3, MPI-ESM-MR, and NorESM1-M. The observed Barents Sea ice extent lies within the ensemble spread of CESM-LE until the recent rapid sea ice loss (Figure 4a). This is consistent with *Vinje* [2001] and *Shapiro et al.* [2003] who found that the sea ice decline during the 1990s was within the range of observed variability during the last 150 years. However, recent winters fall well below the range of simulated variability in CESM-LE.

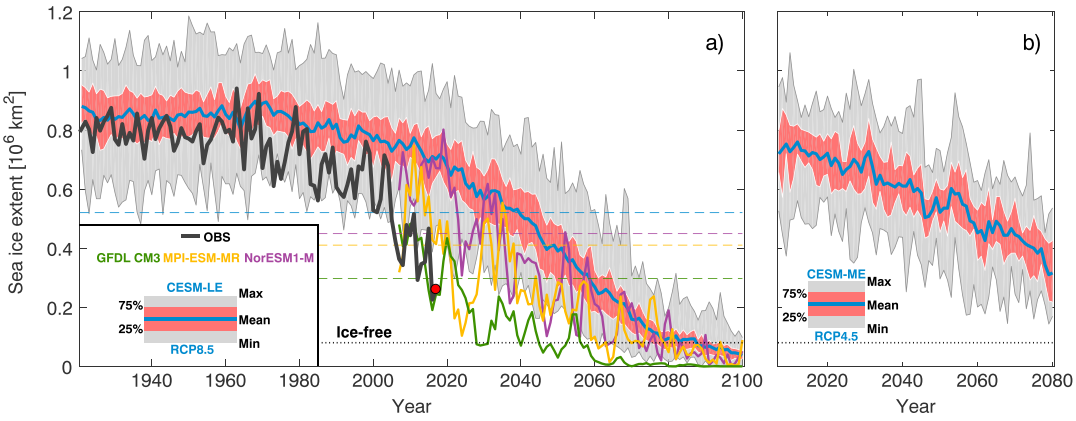

Figure 4. Past, present, and future winter Barents Sea ice extent in the (a) CESM-LE and (b) CESM-ME (ensemble mean: blue line; quartiles: red shading; ensemble spread: gray shading). In Figure 4a the future sea ice extent (2007–2100) is also shown for GFDL CM3 (green), MPI-ESM-MR (yellow), and NorESM1-M (purple). Horizontal dashed lines illustrate the minimum sea ice extent for the corresponding preindustrial control simulations. Observed sea ice variability is shown in black, with the red dot highlighting the winter sea ice extent in 2017. The horizontal dotted black line in Figures 4a and 4b marks (nearly) ice-free conditions, defined as 10% of the 1850–1978 average winter sea ice extent.

All models show a gradually declining sea ice cover toward 2100, with shorter (interannual to decadal) time periods of positive trends also present (Figure 4a). The latter is consistent with decadal-long hiatuses in Arctic sea ice loss as a result of internal climate variability [e.g., *Kay et al.*, 2011; *Swart et al.*, 2015; *Årthun et al.*, 2017]. Ice-free conditions are projected to occur for the first time in 2028 in GFDL CM3, 2061 in MPI-ESM-MR, and 2063 in NorESM1-M. For CESM-LE the range of dates when each ensemble member becomes ice free for the first time is 2061–2088, with a median of 2075, meaning that internal variability leads to a prediction uncertainty of 28 years. Similar uncertainty was found in CESM-LE projections of Arctic summer sea ice [*Jahn et al.*, 2016]. For the ensemble mean, representing the externally forced contribution to future sea ice loss, ice-free conditions occur in 2083. All models suggest that the Barents Sea may become ice free in periods, before recovering due to short-term positive trends. At the end of the century, however, the long-term sea ice loss overrides the periods of positive trends, and the Barents Sea thus remains ice free throughout the year (Figure 4a).

The CESM-LE simulation considers the strong forcing scenario RCP8.5, which assumes that emissions will continue to rise throughout the 21st century [*Moss et al.*, 2010]. The medium forcing scenario RCP4.5, which assumes that emissions peak around 2040, also shows a gradually declining winter Barents Sea ice cover (Figure 4b). However, ice-free winters do not occur in any of the CESM-ME ensemble members before the simulations end in 2080. This highlights that future emissions play an essential role in the further decline of the Barents Sea winter sea ice cover.

6. Discussion and Conclusion

The Arctic summer sea ice extent has decreased dramatically during the last few decades [*Kay et al.*, 2011; *Stroeve et al.*, 2012a; *Overland and Wang*, 2013]. However, recent Arctic sea ice changes are also evident in winter [*Cavalieri and Parkinson*, 2012; *Onarheim et al.*, 2014; *Li et al.*, 2017], and are particularly pronounced in the Barents Sea (Figure 1). Here we have used a new observational data set spanning the time period since 1850 and coupled climate model simulations to assess the uniqueness of the recent winter Barents Sea ice loss and projections for the future. The present winter Barents Sea ice cover is less than a third of the pre-satellite mean. We find that the ongoing Barents Sea ice loss is unprecedented in the historical record (Figure 1c) and an uncommon feature in climate model control simulations (Figure 3). If the most recent 30 year trend persists, simple extrapolation suggests that the Barents Sea might become ice free some time between 2023 and 2036. For a high climate forcing scenario (RCP8.5) the CESM-LE shows ice-free conditions, for the first time, ranging from 2061 to 2088, which is in line with results from MPI-ESM-MR (2061) and NorESM1-M (2063). GFDL CM3 shows ice-free conditions already in 2028, similar to estimates obtained by extrapolating the current observed trend. In contrast, the Barents Sea does not become ice free in the RCP4.5 forced CESM-ME before the end of the simulations in 2080.

The large range in the projected timing of an ice-free Barents Sea (Figure 4) is due to a combination of internal climate variability, model differences, and scenario uncertainty. The intermodel spread in the simulated future Arctic sea ice cover (Figure 4a) [*Stroeve et al.*, 2007; *Kay et al.*, 2011; *Stroeve et al.*, 2012b] might, for instance, be related to differences in the complexity of the sea ice models. *Stroeve et al.* [2007] found that models including more sophisticated sea ice processes were better able to capture the recent observed trend. Similarly, *Bathiany et al.* [2016] argued that the MPI model loses sea ice too quickly in winter due to oversimplified sea ice parametrization. Of the models used here, CESM and NorESM1-M incorporate the relatively sophisticated sea ice model, CICE, but it is not possible to judge based on the results presented here whether these models are more realistic than MPI-ESM-MR and GFDL CM3. Trying to assess which model projection is most reasonable is further complicated by the fact that a realistic representation of the past and present sea ice changes does not imply a correct representation of its future evolution [*Notz*, 2015].

A possible way of reducing the prediction uncertainty is by examining the CESM-LE for emerging constraints that could indicate which trajectory is most reasonable based on the current sea ice state [e.g., *Stroeve and Notz*, 2015; *Notz*, 2015]. We find, however, that the ensemble members in CESM-LE becoming ice free first are not those with small sea ice extent or large sea ice trends at present (and vice versa; not shown), and that we therefore cannot predict which ensemble member becomes ice free first based on the past and present sea ice state. This is consistent with the analysis of the future evolution of the Arctic summer sea ice extent by *Jahn et al.* [2016], which show that common metrics of the past and present sea ice state were unable to reduce the prediction uncertainty from internal variability. As the recent Barents Sea winter sea ice decline has largely been driven by ocean heat transport changes [*Årthun et al.*, 2012; *Onarheim et al.*, 2015; *Li et al.*, 2017], we also examined the predictive skill in Atlantic heat transport (mean, trend, and correlation with sea ice extent) but found no relation to the timing of ice-free conditions (not shown).

The large ensemble spread in CESM-LE projections of future winter sea ice extent indicates that internal variability has a strong influence on the timing of reaching an ice-free Barents Sea. An estimate of the relative contributions of external forcing and internal variability on the most recent sea ice loss can be obtained by comparing the ensemble mean CESM-LE 1988–2017 linear trend with the observed linear trend over the same 30 year time period [cf., *Stroeve et al.*, 2007; *Kay et al.*, 2011]. The averaging across ensemble members cancels out internal variability, and divided by the observed trend, it thus implies the response that results from changes in external forcing. Assuming that the CESM-LE ensemble mean correctly represents the externally forced trend, this calculation indicates that 72% of the recent 30 year trend is due to internal variability. The important role of internal variability is in agreement with *Li et al.* [2017] who found that the observed trend in Barents Sea ice cover during the satellite period has mainly been a result of enhanced ocean heat transport associated with regional internal variability. In summary, internal variability is found to be important for the observed present and modeled future winter sea ice loss in the Barents Sea (Figure 4a). However, modeled internal variability alone cannot explain the recent observed sea ice loss (Figure 3).

Conclusions based on climate model simulations are only as reliable as the model's ability to correctly simulate the governing underlying processes. For the Barents Sea specifically, CMIP5 models generally underestimate ocean heat transport into the Barents Sea and, hence, overestimate the sea ice extent [*Li et al.*, 2017]. Consistently, the models used here also show a slight overestimation, although a comparison with observations is not straightforward as the preindustrial control runs do not include external forcing. *Li et al.* [2017] speculate that these discrepancies are a result of underestimated internal variability in climate models. Consequently, the calculated probability of the current rate of sea ice loss to occur as a result of internal variability (Figure 3) could also be underestimated. The projected timing of ice-free conditions presented here is nevertheless in general agreement with estimates based on downscaled A1B scenarios with a more realistic ocean heat transport and mean sea ice extent [*Smedsrud et al.*, 2013; *Sandø et al.*, 2014b]. However, no detailed analysis of future sea ice loss with respect to past and present trends was performed in these studies.

The recent trend toward less Arctic winter sea ice has predominantly occurred in the Barents Sea (Figure 1), and the Barents Sea could be the first Arctic shelf sea to become ice free year round. With current emissions tracking the RCP8.5 scenario [*Peters et al.*, 2013] the Barents Sea is moving toward ice-free conditions within this century. However, reduced emissions could substantially delay this development (Figure 4). A better understanding of Arctic sea ice variability and trends on different time scales, and the role of internal variability, as provided here, is therefore essential in order to predict future sea ice changes under anthropogenic warming.

Acknowledgments
This research was supported by the Centre for Climate Dynamics (SKD) at the Bjerknes Centre, the University of Bergen, and by the Research Council of Norway through the projects NORTH and PATHWAY. We thank Helene R. Langehaug, Aleksi Nummelin, and two anonymous reviewers for valuable comments that improved the manuscript. We acknowledge the World Climate Research Programme's Working Group on Coupled Modelling, which is responsible for CMIP, and we thank the climate modeling groups for producing and making available their model output. We also acknowledge the CESM Large Ensemble Community Project for making their data available. Observed sea ice concentrations can be downloaded from the National Snow and Ice Data Center; the NASA Team product from November 1978 to February 2017 from http://nsidc.org/data/NSIDC-0051, the near-real-time data for March and April 2017 from http://nsidc.org/data/NSIDC-0081, and the 1850 onward data set, 1850–2013, from http://nsidc.org/data/G10010. We thank the NSIDC for making their data available.

References

ACIA (2005), *Arctic Climate Impact Assessment*, Cambridge Univ. Press, Cambridge, U. K.
Årthun, M., T. Eldevik, L. H. Smedsrud, Ø. Skagseth, and R. B. Ingvaldsen (2012), Quantifying the influence of Atlantic heat on Barents Sea ice variability and retreat, *J. Clim.*, *25*, 4736–4743.
Årthun, M., T. Eldevik, E. Viste, H. Drange, T. Furevik, H. L. Johnson, and N. S. Keenlyside (2017), Skillful prediction of northern climate provided by the ocean, *Nat. Commun.*, *8*, 15875.
Barnhart, K. R., C. R. Miller, I. Overeem, and J. E. Kay (2016), Mapping the future expansion of Arctic open water, *Nat. Clim. Change*, *6*(3), 280–285.
Bathiany, S., D. Notz, T. Mauritsen, G. Raedel, and V. Brovkin (2016), On the potential for abrupt Arctic winter sea ice loss, *J. Clim.*, *29*(7), 2703–2719.
Bentsen, M., et al. (2013), The Norwegian earth system model, NorESM1-M. Part 1: Description and basic evaluation of the physical climate, *Geosci. Model Dev.*, *6*(3), 687–720.
Cavalieri, D. J., and C. L. Parkinson (2012), Arctic sea ice variability and trends, 1979–2010, *Cryosphere*, *6*(4), 881–889.
Cavalieri, D. J., C. L. Parkinson, P. Gloersen, and H. Zwally (1996), *Sea Ice Concentrations From Nimbus-7 SMMR and DMSP SSM/I Passive Microwave Data*, Digital Media, Natl. Snow and Ice Data Center, Boulder, Colo.
Dalpadado, P., K. R. Arrigo, S. S. Hjøllo, F. Rey, R. B. Ingvaldsen, E. Sperfeld, G. L. van Dijken, L. C. Stige, A. Olsen, and G. Ottersen (2014), Productivity in the Barents Sea-response to recent climate variability, *9*(5), e95273.
Giorgetta, M. A., et al. (2013), Climate and carbon cycle changes from 1850 to 2100 in MPI-ESM simulations for the Coupled Model Intercomparison Project phase 5, *J. Adv. Model. Earth Syst.*, *5*(3), 572–597.
Griffies, S. M., et al. (2011), The GFDL CM3 coupled climate model: Characteristics of the ocean and sea ice simulations, *J. Clim.*, *24*(13), 3520–3544.
Jahn, A., J. E. Kay, M. M. Holland, and D. M. Hall (2016), How predictable is the timing of a summer ice-free Arctic?, *Geophys. Res. Lett.*, *43*, 9113–9120, doi:10.1002/2016GL070067.
Kay, J., et al. (2015), The Community Earth System Model (CESM) large ensemble project: A community resource for studying climate change in the presence of internal climate variability, *Bull. Am. Meteorol. Soc.*, *96*(8), 1333–1349.
Kay, J. E., M. M. Holland, and A. Jahn (2011), Inter-annual to multi-decadal Arctic sea ice extent trends in a warming world, *Geophys. Res. Lett.*, *38*, L15708, doi:10.1029/2011GL048008.
Levitus, S., G. Matishov, D. Seidov, and I. Smolyar (2009), Barents Sea multidecadal variability, *Geophys. Res. Lett.*, *36*, L19604, doi:10.1029/2009GL039847.
Li, D., R. Zhang, and T. R. Knutson (2017), On the discrepancy between observed and CMIP5 multi-model simulated Barents Sea winter sea ice decline, *Nat. Commun.*, *8*, 14,991.
Liptak, J., and C. Strong (2014), The winter atmospheric response to sea ice anomalies in the Barents Sea, *J. Clim.*, *27*(2), 914–924.
Maslanik, J., and J. Stroeve (1999), *Near-Real-Time DMSP SSMIS Daily Polar Gridded Sea Ice Concentrations, Version 1*, NASA Natl. Snow and Ice Data Cent. Distrib. Active Archive Cent., Boulder, Colo.
Meier, W., F. Fetterer, M. Savoie, S. Mallory, R. Duerr, and J. Stroeve (2013), *updated 2016, NOAA/NSIDC Climate Data Record of Passive Microwave Sea Ice Concentration, Version 2*, Natl. Snow and Ice Data Cent. (NSIDC), Boulder, Colo.
Meier, W. N., J. Stroeve, and F. Fetterer (2007), Whither Arctic sea ice? A clear signal of decline regionally, seasonally and extending beyond the satellite record, *Ann. Glaciol.*, *46*(1), 428–434.
Miles, M. W., D. V. Divine, T. Furevik, E. Jansen, M. Moros, and A. E. Ogilvie (2014), A signal of persistent Atlantic multidecadal variability in Arctic sea ice, *Geophys. Res. Lett.*, *41*, 463–469, doi:10.1002/2013GL058084.
Moss, R. H., et al. (2010), The next generation of scenarios for climate change research and assessment, *Nature*, *463*(7282), 747–756.
Notz, D. (2015), How well must climate models agree with observations?, *Philos. Trans. R. Soc. A*, *373*(2052), 20140164.
Notz, D., F. A. Haumann, H. Haak, J. H. Jungclaus, and J. Marotzke (2013), Arctic sea-ice evolution as modeled by Max Planck Institute for Meteorology's Earth system model, *J. Adv. Model. Earth Syst.*, *5*(2), 173–194.
Onarheim, I. H., L. H. Smedsrud, R. B. Ingvaldsen, and F. Nilsen (2014), Loss of sea ice during winter north of Svalbard, *Tellus A*, *66*, 23933.
Onarheim, I. H., T. Eldevik, M. Årthun, R. B. Ingvaldsen, and L. H. Smedsrud (2015), Skillful prediction of Barents Sea ice cover, *Geophys. Res. Lett.*, *42*, 5364–5371, doi:10.1002/2015GL064359.
Overland, J. E., and M. Wang (2013), When will the summer Arctic be nearly sea ice free?, *Geophys. Res. Lett.*, *40*, 2097–2101, doi:10.1002/grl.50316.
Peters, G. P., R. M. Andrew, T. Boden, J. G. Canadell, P. Ciais, C. Le Quéré, G. Marland, M. R. Raupach, and C. Wilson (2013), The challenge to keep global warming below 2°C, *Nat. Clim. Change*, *3*(1), 4–6.
Sanderson, B. M., K. W. Oleson, W. G. Strand, F. Lehner, and B. C. O'Neill (2015), A new ensemble of GCM simulations to assess avoided impacts in a climate mitigation scenario, *Clim. Change*, 1–16, doi:10.1007/s10584-015-1567-z.
Sandø, A., Y. Gao, and H. Langehaug (2014a), Poleward ocean heat transports, sea ice processes, and Arctic sea ice variability in NorESM1-M simulations, *J. Geophys. Res.*, *119*, 2095–2108, doi:10.1002/2013JC009435.
Sandø, A. B., A. Melsom, and W. P. Budgell (2014b), Downscaling IPCC control run and future scenario with focus on the Barents Sea, *Ocean Dyn.*, *64*(7), 927–949.
Serreze, M. C., and J. Stroeve (2015), Arctic sea ice trends, variability and implications for seasonal ice forecasting, *Philos. Trans. R. Soc. A*, *373*(2045), 20140159.
Serreze, M. C., M. M. Holland, and J. Stroeve (2007), Perspectives on the Arctic's shrinking sea-ice cover, *Science*, *315*(5818), 1533–1536.
Shapiro, I., R. Colony, and T. Vinje (2003), April sea ice extent in the Barents Sea, 1850–2001, *Polar Res.*, *22*(1), 5–10.
Skagseth, Ø., T. Furevik, R. Ingvaldsen, H. Loeng, K. A. Mork, K. A. Orvik, and V. Ozhigin (2008), Volume and heat transports to the Arctic Ocean via the Norwegian and Barents Seas, in *Arctic-Subarctic Ocean Fluxes*, pp. 45–64, Springer, Dordrecht, Netherlands.
Smedsrud, L. H., et al. (2013), The role of the Barents Sea in the Arctic climate system, *Rev. Geophys.*, *51*, 415–449, doi:10.1002/rog.20017.
Sorokina, S. A., C. Li, J. J. Wettstein, and N. G. Kvamstø (2016), Observed atmospheric coupling between Barents Sea ice and the warm-Arctic cold-Siberian anomaly pattern, *J. Clim.*, *29*(2), 495–511.
Stroeve, J., and D. Notz (2015), Insights on past and future sea-ice evolution from combining observations and models, *Global Planet. Change*, *135*, 119–132.
Stroeve, J., M. M. Holland, W. Meier, T. Scambos, and M. Serreze (2007), Arctic sea ice decline: Faster than forecast, *Geophys. Res. Lett.*, *34*, L09501, doi:10.1029/2007GL029703.
Stroeve, J. C., M. C. Serreze, M. M. Holland, J. E. Kay, J. Malanik, and A. P. Barrett (2012a), The Arctic's rapidly shrinking sea ice cover: A research synthesis, *Clim. Change*, *110*(3), 1005–1027.

Stroeve, J. C., V. Kattsov, A. Barrett, M. Serreze, T. Pavlova, M. Holland, and W. N. Meier (2012b), Trends in Arctic sea ice extent from CMIP5, CMIP3 and observations, *Geophys. Res. Lett.*, *39*, L16502, doi:10.1029/2012GL052676.

Swart, N. C., J. C. Fyfe, E. Hawkins, J. E. Kay, and A. Jahn (2015), Influence of internal variability on Arctic sea-ice trends, *Nat. Clim. Change*, *5*(2), 86–89.

Taylor, K. E., R. J. Stouffer, and G. A. Meehl (2012), An overview of CMIP5 and the experiment design, *Bull. Am. Meteorol. Soc.*, *93*(4), 485–498.

Venegas, S. A., and L. A. Mysak (2000), Is there a dominant timescale of natural climate variability in the Arctic?, *J. Clim.*, *13*(19), 3412–3434.

Vinje, T. (2001), Anomalies and trends of sea-ice extent and atmospheric circulation in the Nordic Seas during the period 1864–1998, *J. Clim.*, *14*(3), 255–267.

Walsh, J. E., W. L. Chapman, and F. Fetterer (2015), *Gridded Monthly Sea Ice Extent and Concentration, 1850 Onward, Version 1*, Natl. Snow and Ice Data Cent. (NSIDC), Boulder, Colo.

Walsh, J. E., F. Fetterer, J. Scott Stewart, and W. L. Chapman (2017), A database for depicting Arctic sea ice variations back to 1850, *Geograph. Rev.*, *107*(1), 89–107.

Zhang, R. (2015), Mechanisms for low-frequency variability of summer Arctic sea ice extent, *Proc. Natl. Acad. Sci.*, *112*, 4570–4575.